Dynamics of charge evolution in glass capillaries for 230-keV Xe^{23+} ions

A. Cassimi,[1] T. Ikeda,[2] L. Maunoury,[3] C. L. Zhou,[1] S. Guillous,[1] A. Mery,[1] H. Lebius,[1] A. Benyagoub,[1] C. Grygiel,[1] H. Khemliche,[4] P. Roncin,[4] H. Merabet,[5] and J. A. Tanis[1,6]

[1]*CIMAP, CEA/CNRS/ENSICAEN/UCBN, BP 5133, F-14070 Caen cedex 5, France*

[2]*Atomic Physics Laboratory, RIKEN, 2-1 Hirosawa, Wako, Saitama 351-0198, Japan*

[3]*GANIL, CEA/CNRS, Boulevard H. Becquerel, BP55027, F-14076 Caen cedex 5, France*

[4]*ISMO, CNRS/Université Paris Sud, Orsay, France*

[5]*Qatar University, P.O. Box 2713, Doha, Qatar*

[6]*Department of Physics, Western Michigan University, Kalamazoo, Michigan 49008, USA*

(Received 31 July 2012; published 4 December 2012)

We have measured the transmission of 230-keV (10-keV/q) Xe^{23+} ions through insulating tapered glass capillaries of microscopic dimensions. The dynamics of charging and discharging processes have been investigated, evidencing an unexpected slow alignment of the beam along the capillary axis. Oscillations of the exiting beam position have been observed during the charging process associated to the formation of charge patches on the capillary inner walls. The emerging ions are guided with a characteristic guiding angle falling on a universal curve proposed for PET polymer nanocapillaries. This result, very similar to the channeling process, is somewhat surprising in view of the significant differences between the straight nanocapillary polymer foils and the tapered microscopic single glass capillary used here. The transmitted ions show no evidence of energy loss or charge changing except for the production of a small neutral fraction that was determined to be due to ions that had become neutralized to form atoms rather than due to photon emission. These results thus test and confirm the validity of transmission and guiding and provide insight into the dynamics of higher-energy ions than have been previously studied in this regard, allowing a determination of the maximum energy for which the guiding process might occur.

DOI: 10.1103/PhysRevA.86.062902 PACS number(s): 61.85.+p, 34.50.Fa, 34.35.+a

I. INTRODUCTION

The study of slow positive ion transmission in insulating nano- and microcapillaries has been actively pursued in recent years [1–8]. It has been proposed that the transmission is due to the formation of self-organized charge patches on the inner walls of the capillaries, thereby inhibiting close collisions of incident ions with the inner capillary surface. This results in no change in the initial charge state or energy loss of the primary beam. This process of Coulomb deflection due to charge patches is called *guiding*, which was first observed by Stolterfoht and co-workers [1]. More recently, evidence for multiple charge patch formation inside the capillaries and the time evolution of these patches has been observed for slow positive ions in nanocapillaries [9,10], manifesting itself in spatial oscillations of about $\pm 1^\circ$ of the transmitted beam around the capillary axis as charge up occurs. While the self-organized charge up of the capillary walls is in fairly good agreement with these observations, the control of this process has not been solved. Investigations involving higher-energy positive ions [6,11] and negative ions [12,13] have also been performed, which do not exhibit guiding so much as transmission. Most of these high-energy studies are centered on the fundamental aspects of the ions or electrons interacting with the capillary, but some have considered possible applications mostly related to creating ~MeV/u well-focused, high-density beams [11] and using these for applications such as in-air particle-induced x-ray emission analysis [14] or radiobiology experiments [15].

In addition to the work with positive ions, some studies have been done for electrons with similar or lower energies (200–1000 eV), on nanocapillary foils [16,17], and for single glass microcapillaries [18–20]. These works show that electrons also are transmitted due to charge up of the capillaries, although the charging by electrons is not as efficient as for slow ions.

In a preliminary report by our group [21], we reported the time evolution of 230-keV Xe^{23+} ions transmitted through a single tapered glass capillary. Changes in the position of the transmitted ions with time have been observed in such capillaries and it was determined that the oscillations observed were caused by multiple charge patches that had built up on the capillary walls during the charging process. After about ~150 nC of charge was deposited on the sample, the position approached equilibrium, indicating that the charge up process was finished.

In the work done here, the results of the preliminary report are extended to investigate the charging and discharging dynamics of the tapered glass capillary with microscopic dimensions (an 800-μm inlet and a 20-μm outlet over a length of a few centimeters). The characteristic guiding angle is determined and the result compared with those previously reported for nanocapillary foils (typical diameters 100 nm and thicknesses of 10 μm, aspect ratio ~100). Strong similarities with the channeling process into crystals are evidenced. Transmitted ions showed no evidence of energy loss or charge changing. However, the output of the capillary showed a small fraction of neutrals that was determined to be due to neutral atoms presumably from ions that had been neutralized after scattering on the walls and then escaped from the capillary. The present results confirm the validity of transmission and guiding for higher-charge state and energy ions.

II. EXPERIMENTAL PROCEDURE

The experiment was performed on the ARIBE beamline at the GANIL facility in Caen, France. A beam of 230-keV Xe^{23+} ions was obtained with an electron cyclotron resonance ion source and was collimated by a 2-mm aperture leading to beam divergence of $\pm 0.23\ \pi$ mm mrad. The capillary alignment with the incident beam was controlled with a goniometer that could position the capillary in both directions transverse to the beam (with 1-μm steps) and in the two rotational directions (with 10^{-3}-degree steps) perpendicular to the beam direction. The capillary holder, which rotated about an axis through the inlet side of the sample, was designed to hold up to six samples at a time. With this holder the samples could easily be positioned in the path of the beam. In the present work, results are reported for a tilt angle of 0.5°. An aluminum screen connected to ground prevented charge up of the capillary entrance and ensured that only ions passing through the sample reached the detector located 650 mm downstream. A specially designed Faraday cup was used for incident current measurements. A total incident current of 60 pA on the beam collimator was used, giving a current of ∼20 pA injected into the capillary through an aperture with a 0.6-mm diameter. To determine the current density of the incident and transmitted ion beams, a 500-μm-thick Au foil with a 10-μm hole in it was placed directly in front of the capillary sample. This foil was used for the current density measurements and not for the actual transmission. The pressure in the sample chamber was about 1×10^{-7} Torr. A schematic of the apparatus is shown in Fig. 1.

The charge states of the emerging beam could be analyzed with a pair of electrostatic parallel plates that enabled dispersion of the components of the outgoing beam onto a position-sensitive detector. This deflector was used to study the neutral fraction that comprised part of the emerging beam. The particle detector consisted of a pair of microchannel plates mounted in a Chevron configuration, placed in front of a delay line anode. The spatial resolution of the detector was determined using the 10-μm pinhole in the Au foil to be better than 70 μm.

The capillaries, made of borosilicate glass (80.95% SiO_2, 12.7% B_2O_3, 2.3% Al_2O_3, and the remainder of Na_2O-K_2O), were made at RIKEN laboratory in Japan. The tapered geometry is created by heating and stretching a section of a glass tube of inner diameter 0.8 mm and an outer diameter of 2 mm. The capillary diameter at the thinnest end of the tube can be made as small as a few micrometers. With a length of a few centimeters and an entrance diameter of ∼800 μm for the present work, the capillary has an equivalent aspect ratio (length/smallest diameter) on the order of about 100 and can thus be viewed as a mechanism to produce very small beams that become enhanced by transmission through the sample.

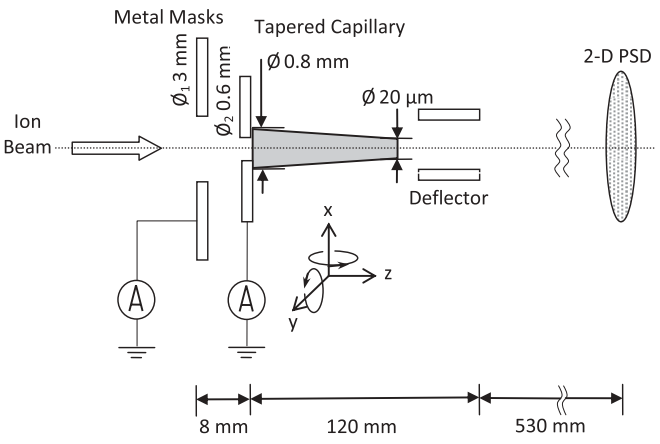

FIG. 1. Schematic of the experimental setup.

The focusing factor is determined from the ratio of the output current density to the input current density. This was obtained by measuring the input and output currents and dividing each value by the area covered by these currents. A focusing factor of three was found for the present case of 230-keV (10-keV/q) Xe^{23+} incident on the tapered capillary, which is somewhat smaller than the value of 10 reported by Ikeda *et al.* [22] for 8-keV Ar^{8+} ions at a 0° tilt angle on a similar tapered capillary. The smaller value in the present case is attributed to the fact that the guiding power, that is, the transmission for nonzero tilt angles, of ions through capillaries decreases as the kinetic energy of the ions increases, as is discussed below. For a tilt angle of 0° the transmission has been noted to increase with ion kinetic energy [23]. While a scan of the angle between the beam axis and the capillary axis has been performed to obtain the characteristic angle ψ_c (see Sec. III B), most of the presented results have been obtained at an angle of 0.5°, for which a surprising behavior of the outgoing beam has been observed.

III. RESULTS AND DISCUSSION

Here we present the charging and discharging dynamics for the transmission of 230-keV Xe^{23+} ions through a single tapered glass capillary, followed by a discussion of the characteristic guiding angle. We then present a determination of the neutral component in the emerging beam and the evidence that it is due to neutral atoms rather than to photons.

A. Charging and discharging dynamics

Charging and discharging curves for the capillary used in the present work are shown in Figs. 2 and 3, respectively, for a tilt angle of 0.5°. The beam was first put on the capillary when it was initially uncharged. Figure 2 shows a rather abrupt rise of the transmitted intensity lasting about 10 min, followed by a quiet period lasting about the same time. Then the sample begins to charge up smoothly. The charge was still increasing at about 2 h when the beam had to be turned off. However, the characteristic charging value appears to be in the neighborhood of 120 nC (=6000 s = 100 min). For the discharging curve of Fig. 3, the behavior seems to be typical of those previously observed and is considerably faster than the charging time. The discharge time depends only on the material properties while the charging time depends also on the injected beam current. These results are difficult to compare quantitatively with nanocapillary samples having an aspect ratio of ∼100 that have typically been done for lower energies ions such as 3-keV Ne^{7+} at tilt angles of 3° or higher (see, e.g., Ref. [24]), which resulted in charging constants of 100 nC or more deposited on these samples. Surprisingly, in spite of the large differences

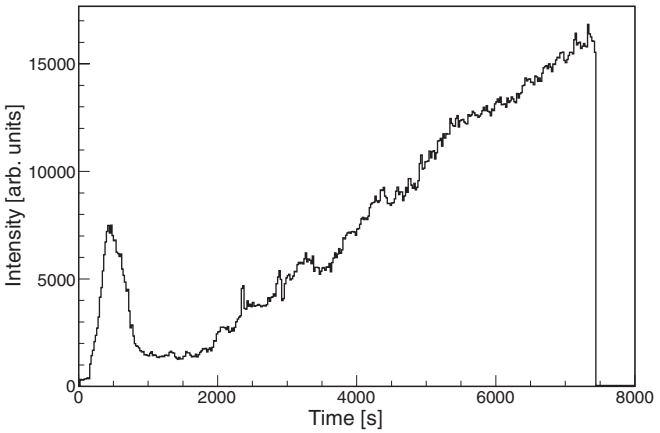

FIG. 2. Charging of the capillary as a function of the deposited charge for 230-keV (10-keV/q) Xe^{23+}. The current injected into the capillary was ∼20 pA. The corresponding times are shown for convenience. The fitted exponential curve gives a characteristic charging value of ∼120 nC (=6000 s = 100 min).

in material (glass vs PET), in geometry (tapered vs straight), and dimension (μm vs nm), as well as tilt angle, the charge deposited is very similar.

A question arises as to the origin of the sudden large initial increase of the charging curve followed by the rather fast decrease after a short interval in Fig. 2. This initial rise is attributed to the buildup of the primary charge patch at the entrance to the capillary, which causes the transmission to occur quickly. The decrease follows the deposition of more

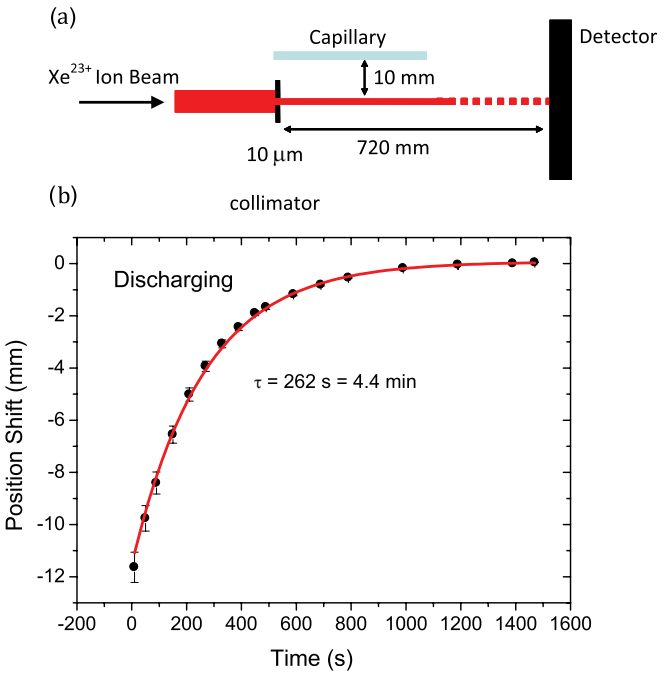

FIG. 3. (Color online) Measurement of the discharge of the sample. (a) Schematic of experimental setup; (b) discharge curve for the capillary as a function of time. In panel (a) it is seen that no beam had to be put on the capillary to measure the discharge. The fitted exponential curve to the discharge in panel (b) gives a time constant of 262 s (=4.4 min).

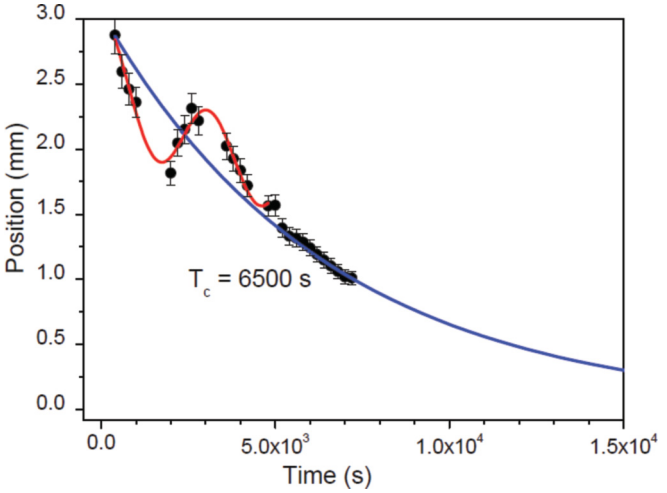

FIG. 4. (Color online) Position of the transmitted beam as a function of time. Plotted are the following: solid circles, present data; blue (dark gray) curve, overall exponential decrease showing the approach to equilibrium; red (light gray) curve, oscillatory behavior, consisting of a cosine function convoluted with an exponential function, of the transmitted beam. The position is measured from the capillary axis for the tilt angle of 0.5°, with zero being along the axis of the capillary. It is seen that the beam lies entirely on one side of the capillary during the transmission and approach to equilibrium. The charging time found for this curve from fitting the oscillatory function to it is ∼6500 s, which is equivalent to a charging value of 130 nC. This is to be compared with 120 nC, as found in Fig. 2.

charge in this region, causing the transmitted beam to be deflected too much, thus inhibiting transmission. However, after a short while the transmission begins again as a subsequent charge patch is developed and the beam can then go through the capillary once again. After this, the transmission continuously increases, indicating that now the charge patches are developed to the point where there is rising transmission as equilibrium is approached. This behavior is confirmed in Fig. 4, which shows oscillations of the position of the beam, with an amplitude of about 500 μm, as a function of the time (charge) elapsed. These oscillations have been observed previously [9,10] and attributed as well to the charge patch creation.

Unfortunately, it is not possible to determine from Figs. 2 and 4 how many charge patches exist inside the capillary, but it can be deduced from the position of the beam when the transmission approaches equilibrium that the number is even, with a minimum value of two. It is observed from Fig. 4 that the transmission goes through smaller oscillations, causing the transmitted intensity to change direction on its overall path, with this path always off the capillary axis on the same side and approaching the axis as the transmission goes to equilibrium. These smaller oscillations, due to the building up of additional charge patches, are damped with time as the charge up increases, indicating that the patches become sufficient to transmit the beam without interruption, while continuing to charge the sample until a steady state is reached. At a value of ∼150 nC deposited into the sample (Fig. 2) the oscillations appear to have ended, and from the beam position plot of Fig. 4 it is shown that the beam exponentially

approaches the capillary axis (indicated by zero on the axis). This curve is characterized by a charging value of 130 nC, which is in good agreement with the value of 120 nC obtained from Fig. 2. Alignment of the beam direction with the capillary axis, while being off axis for the duration of transmission, has not been observed up to now and indicates the diffusion of charge along the inner surface of the capillary as the beam continues to deposit charge.

These two contributions to the beam deflection, fast damped oscillations and slow exponential deflection towards the axis, can be attributed, respectively, to the dynamics of charge patch creation which causes the beam to oscillate back and forth and to the diffusion dynamics of the charge patches on the capillary wall that slowly tend to align the beam on the capillary axis. The latter is because of the high resistivity of borosilicate and has not been observed previously. The reason that this was observed in the present work might be due to the length of single capillaries to provide enough room to have well-separated patches produced on their inner walls. Then, from the different effects of these two processes on the beam, they can be discriminated from one another.

The discharging curve for the sample in Fig. 3 shows a much shorter time of 262 s (about 4.4 min), and this curve was obtained by never having to put the beam on the sample to measure it. Instead, as seen in the figure, the deflection of the microbeam was measured by projecting it parallel to the capillary axis with the axis at a distance of about 10 mm from it. This was done until the beam was no longer deflected, as seen in the inset. This allowed the entire curve to be obtained without interruption and also without reintroducing the beam into the capillary to measure the amount of charge on the walls, an effect that puts some additional charge on the sample in the process of measuring it. The obtained discharge time value, which depends only on the material resistivity, either through the surface or through the bulk, is in very good agreement with a recent theoretical calculation [25] predicting a discharge time of 240 s.

Much the same can be said about the width values of the exiting beam shown in Fig. 5. Here, the width starts out at its narrowest value and then slowly increases to a final equilibrium value, nearly doubling its initial value with a time constant of about 5130 s (∼85 min), as obtained from an exponential fit to the data. The reason for the increase in width can be attributed to the beam having its narrowest width at the beginning of transmission and then becoming broader as the exit of the capillary starts to charge up. The more the exit of the capillary charges up, the more lateral deflection the exiting ions will experience and, hence, the increase in the width. The width broadening slows down as the sample becomes charged up, and approaches its equilibrium value as the sample reaches equilibrium charge. The time constant for this change is somewhat less than the estimated charging time of ∼6000 s (100 min) from Figs. 2 and 4 and is probably reasonable because the width is likely not to be as sensitive to changes in the capillary charge build up as is the intensity. The width is instead mostly sensitive to the charge at the exit. The increase in width by a factor of two in these data is quite large and represents a substantial amount of charge inside the capillary. Even when the position of the beam turns around, the width does not adjust to this change because of the continuous charging of the exit of the capillary as it approaches equilibrium.

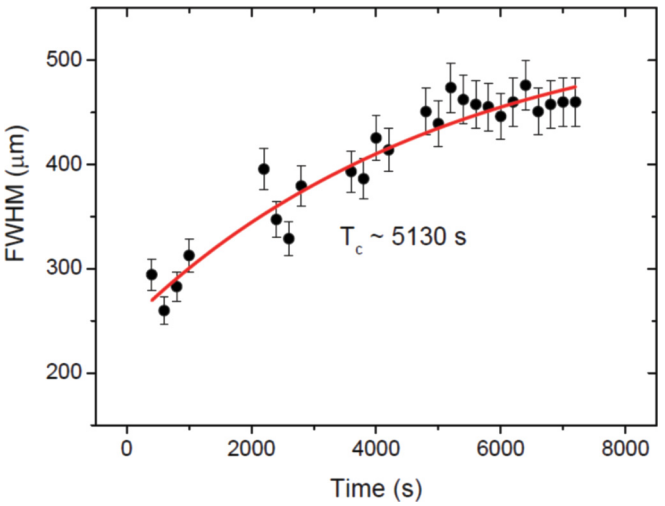

FIG. 5. (Color online) Full width at half maximum (FWHM) in μm as a function of time. The solid circles represent the data while the red curve is an exponential fit to the data. The FWHM is seen to approach equilibrium in less time than the position curve shown in Fig. 4. Since the FWHM is attributed mainly to the charge collected at the exit, it is not related to the same charging time that determines the position.

B. Universal scaling of the guiding at equilibrium

Much previous data have been collected for nanocapillaries and the question here is how the present data fit into the guiding scheme of these data. In the present case, the capillary is glass instead of PET and its diameter is much larger (on the micrometer scale), with the entrance and exit openings not having the same size because of the tapered shape of the capillary compared to the straight cylindrical capillaries that were used for the PET nanocapillaries [1,2].

With regard to PET, Stolterfoht *et al.* [2] have developed a model for nanocapillaries in which the *characteristic guiding angle*, for which the transmitted intensity drops by a factor of $1/e$ from its initial value, can be scaled in terms of the projectile energy divided by charge. This guiding angle can be determined by rotating the capillary and measuring the intensity for each angle. The characteristic guiding angle is related to the maximum transverse energy that is opposed by the electric potential energy of the charged walls of the capillary. To arrive at an expression, it is noted that the perpendicular velocity $v_\perp$ of the incoming beam to the capillary wall is given by $v_\perp = v \sin\psi$, where v is the incident velocity and ψ is the tilt angle of the sample. This gives a transverse energy of $E_\perp = E \sin^2\psi$, with $E_\perp$ and E the perpendicular and total energy of the incident beam, respectively. Then, the maximum transverse energy is related to the characteristic guiding angle and the mean electric potential energy V_m that exists on the capillary walls such that

$$E_{\perp\max} = E \sin^2\psi_c = qV_\mathrm{m} \quad (1)$$

or

$$\sin^2 \psi_c = q V_m / E, \tag{2}$$

where q is the electric charge. Since we are dealing with very small angles, this can be written as

$$\sin^2 \psi_c \simeq \psi_c^2 = q V_m / E. \tag{3}$$

This formulation is very similar to the channeling process in crystals for which such a characteristic angle, usually called the critical angle, fixing the channeling conditions, is given for that process by screened potential of the atomic rows [26] that deflects and guides the beam along the crystal subnanochannels.

The tilt angle distributions could be fit with the Gaussian-like function [2],

$$\frac{dY}{d\Omega} = \frac{dY_{\max}}{d\Omega} \exp\left(-\frac{\sin^2 \psi}{\sin^2 \psi_C}\right), \tag{4}$$

where Y and $Y_{\max}$ are the intensity at a given tilt angle ψ and the maximum intensity, respectively, while ψ_c is a fitting parameter. Then, by measuring the guiding angle as mentioned above, a universal plot can be made for $\sin^2 \psi_c$ (or ${\psi_c}^2$) as a function of q/E, where it is assumed that V_m has a fixed and constant value. For convenience, ψ_c has been plotted as a function of $(q/E)^{1/2}$, that is, the square root of q/E as shown in Fig. 6. The slope of this line in conjunction with Eq. (3) gives the mean electric potential of the capillary wall without any assumed potential shape across the capillary. From the slope a value of ~5.1 V is obtained.

In the plot of Fig. 6, data from Ref. [2] for Ne^{7+}, Ne^{9+}, Ar^{9+}, Ar^{13+}, and Xe^{25+} with energies ranging from 3 to 40 keV transmitted through PET nanocapillaries are exhibited with our point for 230-keV Xe^{23+}. This point for Xe^{23+} that corresponds to the highest energy is seen to be well represented by the universal curve from Eq. (3). This result is quite surprising

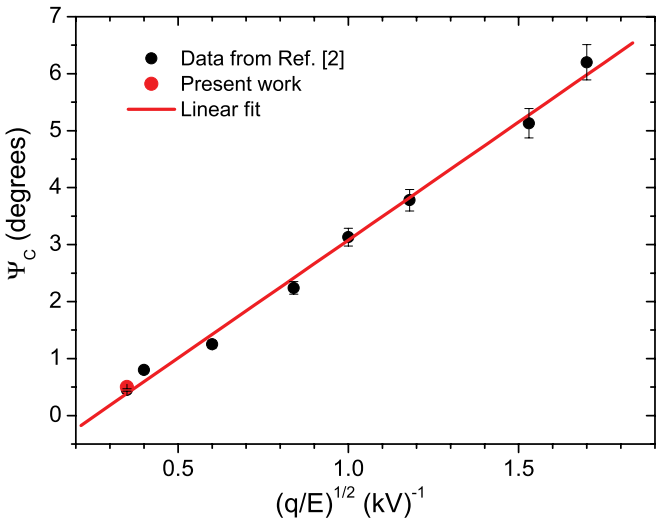

FIG. 6. (Color online) Characteristic angle Ψ_c as a function of $(q/E)^{1/2}$, where q and E are the incident charge and energy (in keV), respectively (see scaling curve: red (light gray) line, developed from earlier PET data for various ions Ref. [2]). Data are as follows: solid black circles, PET data; solid red (light gray) circle, present work.

in view of the large differences in the capillary geometry and dimension (nanometer sized for PET versus micrometer sized for glass capillary). Thus, the curve shows that the ion guiding power is not sensitive to the insulating material the capillary is made from or to the shape or to the outlet dimensions of the capillary within the nanometer to micrometer scale. This result shows that the maximum potential seen by the ions and induced by the charge deposited on the capillary wall is constant whatever the material or the shape of the capillary. Instead, the curve demonstrates that the capillary guiding power, as measured by the characteristic angle, decreases quite strongly as the ion energy increases. This makes sense as the rigidity of the beam increases with energy while the maximum charge the capillary may hold seems to be limited. We can thus derive the important conclusion that the guiding power of a capillary depends neither on its shape nor the material it is made from. Things that do depend on these characteristics are the transmission factor as well as the characteristic time constants involved in the charging and discharging of the capillary walls.

C. Neutral fraction of the transmitted beam

When slow ions are transmitted through nano- or micro-capillaries it has usually been found that nearly all of the transmitted ions remain in the incident charge state, and there is very little charge exchange [1]. However, recently it was found that a small fraction of Ar neutrals was formed in the incidence of 3-keV Ar^{7+} ions on PET nanocapillaries at a tilt angle of 5.5° and accompanied the emerging Ar^{7+} ions [27]. In this work, the neutral fraction was found to be about 1%–2% of the Ar^{7+} fraction, and, furthermore, this neutral fraction reached equilibrium three or four times faster than the ion fraction. The main conclusion from this work was that the emission of neutrals occurs before the ions are guided, showing that charge patch formation starts with the formation of neutrals and the subsequent emission of some of these.

In the present work, a similar neutral fraction, though somewhat larger, was associated with the transmission of 230-keV Xe^{23+} ions through the tapered glass capillary used here. It was not assumed, however, that the transmitted fraction consisted of atoms, and thus the possibility of photons was also considered. A typical intensity spectrum for this effect at a tilt angle of 0.5° is shown in Fig. 7. This spectrum was created from the two-dimensional information that was collected on the position-sensitive detector by projecting the beam horizontally through the electrostatic deflector plates that follow the sample scattering region. In the figure we see a strong sharply peaked signal from the Xe^{23+} component (deflected) and a much smaller contribution (not deflected) covering a broad distribution for the neutrals or photons. The spectrum shows a neutral fraction that is only 1% or 2% of the intensity of Xe^{23+} at its maximum value, but because of its much broader width it amounts to about 10% the intensity of Xe^{23+}. This higher proportion of the neutral fraction is likely due to the lower resistivity, about two to three orders of magnitude, of the tapered glass capillaries compared to PET nanocapillaries. A method of investigating this would be to measure the temperature dependence of the transmission as

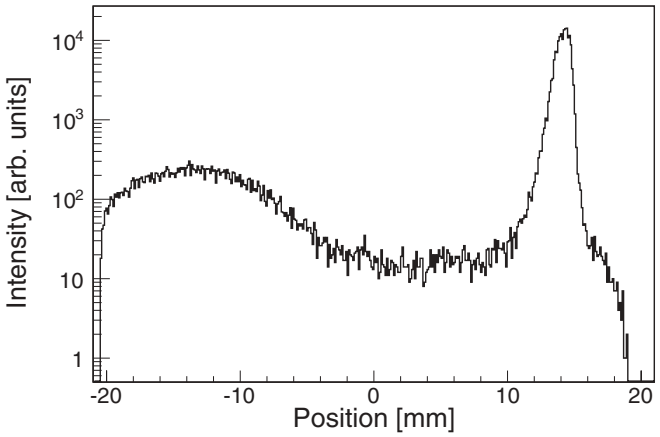

FIG. 7. Spectra showing logarithmic plot of the main beam of Xe^{23+} ions detected and a smaller (∼10%) neutral contribution determined to be due to incident ions that were neutralized and then exited the capillary. This spectrum was obtained by deflecting the main beam with the deflector plates installed following interaction with the capillary. The neutral contribution is noted to be much broader than the incident ions.

the glass capillary is heated [8], which should then give rise to an even higher proportion of neutrals that are formed.

To determine whether the particles are neutrals or photons, we present in Fig. 8 a pulse height analysis of the output of the microchannel plate detector for both the transmitted Xe^{23+} beam [Fig. 8(a)] and the neutral spot [Fig. 8(b)] at this position when the beam is deflected. Here we see that the pulse height analysis of the neutral fraction in Fig. 8(b) gives about the same shape and occurs at the same pulse height as the main beam [Fig. 8(a)]. For photons, the expected shape for the pulse height distribution is a decreasing exponential, which is the reason for their poor detection efficiency by MCPs. Hence, we are led to conclude that the neutral fraction consists of ions that have become neutralized rather than being due to photons. It is noted that in Ref. [27] the same conclusion was reached also with no intermediate charge states between the main beam and the neutral fraction.

Finally, it must be argued why a neutral beam fraction is formed without any intermediate charge states. Juhász *et al.* [27] explained this by the neutral fraction being formed early in the charging process when there is little charge deposited to prevent the incoming ions from striking the capillary walls. Then, as the charge builds up the neutral fraction reaches equilibrium more quickly, which was measured to be three or four times faster by these authors. Therefore, the production of more neutrals is largely inhibited. Instead, the majority of incoming ions are now deflected at larger distances, thus avoiding collisions with the capillary walls. The incident ions are unaffected by wall collisions and those that are transmitted come out with no charge change. This also explains why there are essentially no intermediate charge states because those ions that become neutralized "dive" further into the bulk and form the well-known hollow atoms when they interact with surfaces due to the strong efficiency of surfaces to neutralize ions. Thus, the neutral beam spot in the present work is attributed to atom formation without producing intermediate charge states by the same mechanism as in the work of Ref. [27]. In the present

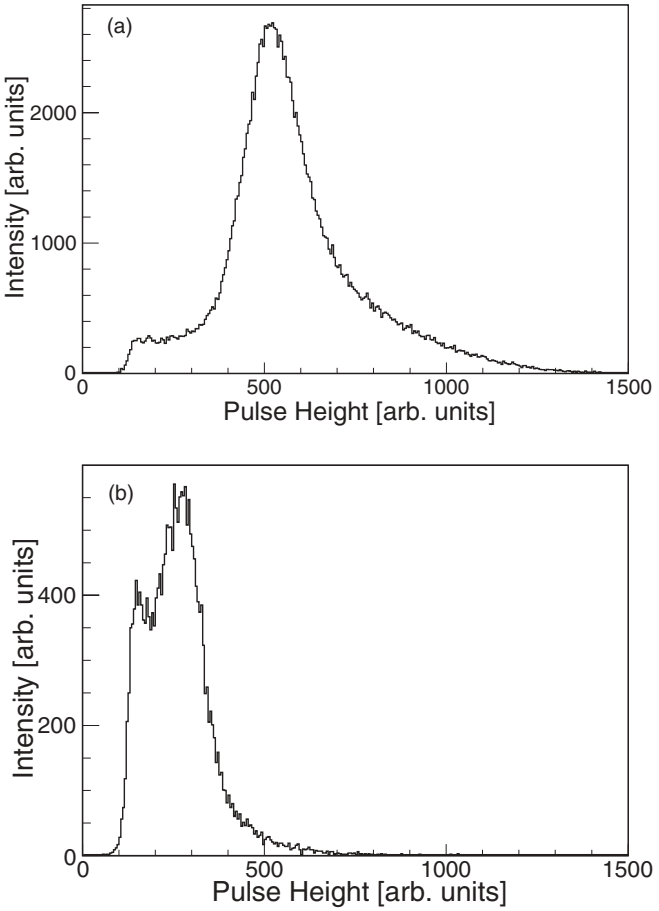

FIG. 8. Pulse-height analysis spectra for the main beam (a) and the neutral fraction (b). The similar behavior of the two spectra led to the conclusion that the neutral fraction was particles rather than photons.

case we note again, however, that this is for a very different sample made of glass rather than PET and having much larger and unequal inlet and outlet dimensions.

IV. CONCLUSION

Results for slow 230-keV (10-keV/q) Xe^{23+} ions transmitted through an insulating tapered glass capillary tilted at 0.5° to the beam have been presented. The charging curve shows about 120 nC (=6000 s = 100 min) of charge (time) required for this, while discharging takes only about 262 s (=4.4 min) of time. The charging time depends strongly on the value of the injected ion current. The charging time is comparable to results obtained for PET foils, although no direct comparison can be made because those samples have been measured for significantly larger tilt angles (about 3° and 5°) and they have been studied for considerably lower energy ions. Also, the PET foils were nanocapillaries so it is not possible to make a direct comparison with these samples.

A surprising result of the charging curve was the burst of intensity that appeared initially and then decreased after about 10 min to nearly zero. These changes in intensity were attributed to the changes in the beam position due to the fast buildup of the first charge patch inside the capillary. From

the subsequent changes in position and the final position of the transmitted ions approaching the capillary axis, it was determined that an even number of charge patches were formed but the actual number could not be determined. The width of the transmitted beam also increased significantly, by about a factor of two, but it did not give any further information on the number of charge patches. The width evolution had a time constant of about 4400 s (∼70 min) as it approached equilibrium, which is about two-thirds of the value for charging the capillary. The primary observations are that two behaviors have been evidenced. Oscillations of the beam are attributed to the charge patch creation dynamics, while the slow alignment of the beam along the capillary axis is due to the charge patch diffusion dynamics on the capillary walls.

The characteristic guiding angle, that is, the tilt angle at which the transmitted intensity falls to $1/e$ of its initial value, was determined and the point put on a universal scaling curve with previous measurements. In this scaling law the characteristic angle is predicted to follow a universal curve as a function of $(q/E)^{1/2}$ that follows a straight line. The data point from the present work fits well on this curve and served to substantiate this scaling for a much wider range of beam energies and a very different sample. Previously, the law had been tested only for polymer nanocapillaries that were straight, but not for glass capillaries of microscopic size and which were not straight. So, in addition to verifying the law for a higher energy, the present results also show that it does not particularly depend on the material of the capillary, its shape, or the dimensions of it. The present data point verifies that the transmission decreases quite strongly with beam energy and demonstrates that the guiding power decreases quite strongly with the incident beam energy, as expected. The present energy of 230 keV for Xe^{23+} is shown to be close to the maximum for which guiding is expected to be possible as the critical angle is largely reduced.

Finally, the question as to the origin of a smaller neutral fraction (about 10%) that was found in the transmitted beam was answered. When the emerging beam from the sample was separated into its component charge states with electrostatic deflector plates, no other intermediate charge states between that of the incident beam and the neutral fraction were observed. The beam profile of the neutral fraction showed a much broader width, about six to seven times as much, as the width of the main beam. It was believed that this component could be due to photons or to neutral atoms. A pulse height analysis of detector signals of the main beam and neutral fractions showed the pulse heights to be the same. Hence, it was concluded that the neutral fraction must be due to atoms rather than to photons, since the latter are not expected to have a pulse height distribution the same as particles and should be significantly smaller and merge with the noise. This was not seen.

The only remaining question then was the fact that there were no other charge states visible between the main beam Xe^{23+} and the neutral fraction. This was attributed to the fact that the neutral fraction equilibrates considerably faster than the main beam fraction and hence contributes to the charging of the patch. While doing this, these ions are not shielded from interactions with the capillary walls and are easily neutralized in these ion-surface interactions which are known to efficiently neutralize ions. In becoming neutralized, some of these atoms find their way to the capillary exit and appear as scattered particles, and thus other charge states are not created in this process.

The results presented here provide a rather complete study for the highest energy and charge state of the transmission of low-energy heavy ions through a tapered glass capillary. Future studies are planned for different beams with still higher charge states of varying energies for other tapered capillaries and conical capillaries as well. All in all, this work should provide a basis for the fundamental understanding of low-energy highly charged ions passing through insulating capillaries of microscopic dimensions.

ACKNOWLEDGMENTS

The authors wish to thank the CIMAP staff for their excellent technical support. C. L. Zhou was supported by the International Graduate Scholarship Program (IGSP) from the China Scholarship Council. J.A.T. was supported by a grant from the Basse-Normandie region (Convention No. 11P01476) and from the European Union through its FEDER fund (Grant No. 32594).

[1] N. Stolterfoht, J. H. Bremer, V. Hoffmann, R. Hellhammer, D. Fink, A. Petrov, and B. Sulik, Phys. Rev. Lett. **88**, 133201 (2002).

[2] N. Stolterfoht, R. Hellhammer, J. Bundesmann, and D. Fink, Phys. Rev. A **77**, 032905 (2008).

[3] N. Stolterfoht, R. Hellhammer, Z. Juhász, B. Sulik, V. Bayer, C. Trautmann, E. Bodewits, A. J. de Nijs, H. M. Dang, and R. Hoekstra, Phys. Rev. A **79**, 042902, (2009).

[4] M. B. Sahana, P. Skog, G. Vikor, R. T. Rajendra Kumar, and R. Schuch, Phys. Rev. A **73**, 040901(R) (2006).

[5] H. F. Krause, C. R. Vane, and F. W. Meyer, Phys. Rev. A **75**, 042901 (2007).

[6] T. Ikeda, Y. Kanai, T. M. Kojima, Y. Iwai, Y. Kanazawa, M. Hoshino, T. Kobayashi, G. P. Pokhil, and Y. Yamazaki, J. Phys.: Conf. Ser. **88**, 012031 (2007).

[7] A. Cassimi, T. Muranaka, L. Maunoury, H. Lebius, B. Manil, B. A. Huber, T. Ikeda, Y. Kanai, T. M. Kojima, Y. Iwai, T. Kambara, Y. Yamazaki, T. Nebiki, and T. Narusawa, Int. J. Nanotechnol. **5**, 809 (2008).

[8] R. J. Bereczky, G. Kowarik, F. Aumayr, and K. Tőkési, Nucl. Instrum. Methods Phys. Res., Sect. B **267**, 317 (2009); R. J. Bereczky, G. Kowarik, C. Lemaignan, A. Macé, F. Ladinig, R. Raab, F. Aumayr, and K. Tőkési, *AIP Conference Proceedings*, Vol. 1336 (AIP, New York, 2011), pp. 119–122.

[9] P. Skog, H. Q. Zhang, and R. Schuch, Phys. Rev. Lett. **101**, 223202 (2008); H.-Q. Zhang, P. Skog, and R. Schuch, Phys. Rev. A **82**, 052901 (2010).

[10] Y. Kanai, M. Hoshino, T. Kambara, T. Ikeda, R. Hellhammer, N. Stolterfoht, and Y. Yamazaki, Phys. Rev. A **79**, 012711 (2009).

[11] T. Nebiki, T. Yamamoto, T. Narusawa, M. B. H. Breese, E. J. Teo, and F. Watt, J. Vac. Sci. Technol. A **21**, 1671 (2003).
[12] G. Sun, X. Chen, J. Wang, Y. Chen, J. Xu, C. Zhou, J. Shao, Y. Cui, B. Ding, Y. Yin, X. Wang, F. Lou, X. Lv, X. Qiu, J. Jia, L. Chen, F. Xi, Z. Chen, L. Li, and Z. Liu, Phys. Rev. A **79**, 052902 (2009).
[13] L. Chen, Y. Guo, J. Jia, H. Zhang, Y. Cui, J. Shao, Y. Yin, X. Qiu, X. Lv, G. Sun, J. Wang, Y. Chen, F. Xi, and X. Chen, Phys. Rev. A **84**, 032901 (2011).
[14] T. Nebiki, M. H. Kabir, and T. Narusawa, Nucl. Instrum. Methods Phys. Res., Sect. B **249**, 226 (2006).
[15] Y. Iwai, T. Ikeda, T. M. Kojima, Y. Yamazaki, K. Maeshima, N. Imamoto, T. Kobayashi, T. Nebiki, T. Narusawa, and G. P. Pokhil, Appl. Phys. Lett. **92**, 023509 (2008).
[16] A. R. Milosavljević, G. Vikor, Z. D. Pešić, P. Kolarž, D. Šević, B. P. Marinković, S. Mátéfi-Tempfli, M. Mátéfi-Tempfli, and L. Piraux, Phys. Rev. A **75**, 030901(R) (2007).
[17] S. Das, B. S. Dassanayake, M. Winkworth, J. L. Baran, N. Stolterfoht, and J. A. Tanis, Phys. Rev. A **76**, 042716 (2007).
[18] B. S. Dassanayake, S. Das, R. J. Bereczky, K. Tőkési, and J. A. Tanis, Phys. Rev. A **81**, 020701(R) (2010).
[19] B. S. Dassanayake, R. J. Bereczky, S. Das, A. Ayyad, K. Tőkési, and J. A. Tanis, Phys. Rev. A **83**, 012707 (2011).
[20] S. J. Wickramarachchi, B. S. Dassanayake, D. Keerthisinghe, A. Ayyad, and J. A. Tanis, Nucl. Instrum. Methods Phys. Res., Sect. B **269**, 1248 (2011).
[21] A. Cassimi, L. Maunoury, T. Muranaka, B. Huber, K. R. Dey, H. Lebius, D. Lelièvre, J. M. Ramillon, T. Been, T. Ikeda, Y. Kanai, T. M. Kojima, Y. Iwai, Y. Yamazaki, H. Khemliche, N. Bundaleski, and P. Roncin, Nucl. Instrum. Methods Phys. Res., Sect. B **267**, 674 (2009).
[22] T. Ikeda, Y. Kanai, T. M. Kojima, Y. Iwai, T. Kambara, Y. Yamazaki, M. Hoshino, T. Nebiki, and T. Narusawa, Appl. Phys. Lett. **89**, 163502 (2006).
[23] R. Hellhammer, P. Sobocinski, Z. D. Pešić, J. Bundesmann, D. Fink, and N. Stolterfoht, Nucl. Instrum. Methods Phys. Res. B **232**, 235 (2005).
[24] N. Stolterfoht, R. Hellhammer, Z. Juhász, B. Sulik, E. Bodewits, H. M. Dang, and R. Hoekstra, Phys. Rev. A **82**, 052902 (2010).
[25] T. Schweigler, C. Lemell, and J. Burgdörfer, Nucl. Instrum. Methods Phys. Res., Sect. B **269**, 1253 (2011).
[26] D. S. Gemmell, Rev. Mod. Phys. **46**, 129 (1974).
[27] Z. Juhász, B. Sulik, R. Rácz, S. Biri, R. J. Bereczky, K. Tőkési, Á. Kövér, J. Pálinkás, and N. Stolterfoht, Phys. Rev. A **82**, 062903 (2010).